buildings

Article

Numerical Simulation of the Blast Resistance of SPUA Retrofitted CMU Masonry Walls

Yi Zhang [1], Jiahui Hu [2,*], Wenda Zhao [3,*], Feng Hu [1] and Xiao Yu [1]

1 Institute of Defense Engineering, AMS, PLA, Beijing 100850, China
2 College of Civil Engineering, Tongji University, Shanghai 200092, China
3 China Construction Engineering Bureau Co., Ltd., Shanghai 200122, China
* Correspondence: hujiahui@tongji.edu.cn (J.H.); zhaowenda@cscec.com (W.Z.)

Abstract: Through numerical simulation, the blast-resistant performance of spray polyurea elastomer (SPUA) retrofitted concrete masonry unit (CMU) masonry infill walls under far-range blast loading was studied. From an engineering perspective, the effects of boundary conditions and thickness of a SPUA layer on enhancing the blast resistance of masonry infill walls are discussed, and the blast resistance of SPUA-retrofitted and grouted CMU masonry infill walls are compared. It is concluded that the boundary constraint conditions and the anchorage length of SPUA layer have limited improvement on the blast-resistant performance of the wall; the thickness of SPUA layer can significantly improve the blast-resistant performance of the wall as the blast loading increases. In addition, SPUA retrofitting shows relatively better performance to reinforce masonry infill walls.

Keywords: far-range explosion; numerical simulation; masonry walls; sprayed polyurea; dynamic response

check for updates

Citation: Zhang, Y.; Hu, J.; Zhao, W.; Hu, F.; Yu, X. Numerical Simulation of the Blast Resistance of SPUA Retrofitted CMU Masonry Walls. *Buildings* **2023**, *13*, 446. https://doi.org/10.3390/buildings13020446

Received: 14 November 2022
Revised: 30 November 2022
Accepted: 9 December 2022
Published: 6 February 2023

1. Introduction

Masonry walls are widely used around the world because of the high performance, low cost, and easy accessibility. Ettouney et al. [1] estimated that more than 70% of the world's existing buildings are masonry structures, in addition to which the majority of building envelopes are still dominated by masonry infill walls. ABS blast consultants [2] found that up to 75% of the people killed or injured in terrorist attacks from the explosion of windows, doors, glass, and walls, experienced secondary injuries from flying debris. Relevant codes clearly state that the use of unreinforced masonry walls is prohibited on new building facades, and for existing buildings, effective blast mitigation measures should be taken to achieve the same level of protection.

At present, the mainstream blast-resistant reinforcement for existing masonry structures includes: blast walls and other isolation devices, light steel keel reinforcement, external steel plate reinforcement, external lightweight sacrificial layer reinforcement, and external spray (coating) elastic polymer material reinforcement. Since the late 1990s, based on the need for blast-resistant reinforcement of human defense buildings in warfare, foreign military research institutions and scholars began research work in related fields. Davidson et al. [3–7] from the U.S. Air Force Research Laboratory (AFRL) first conducted extensive tests, numerical simulations, and theoretical research work on the dynamic response and damage of 53 polymers and their composites (including plastic sheets, polyurethane, brush-coated materials, sprayed polyurea, etc.) on reinforced small concrete hollow block one-way masonry walls under lateral blast loads. The results showed that the use of polyurea-like materials to reinforce masonry walls can effectively reduce the generation of block fragments and mitigate the degree of wall damage, enhancing the blast resistance of masonry walls. Subsequently, researchers from around the world [8–13] also conducted studies on the blast resistance of spray polyurea elastomer (SPUA) retrofitted masonry walls. By conducting blast tests, Li et al. [14] concluded that the basalt fiber reinforced polymer (BFRP) strips could reduce the number of fragments for masonry walls subjected to gas explosions. However, since the peak overpressure acting on the walls may increase due to the growing blast resistance of the back surfaces, the splash distance of debris could be larger, which deprives some of the effectiveness of protecting the safety of people inside the building.

In the study of masonry wall blast resistance, Varma et al. [15] conducted blast tests on 27 pieces of 3 m $\times$ 3 m common clay brick walls under a variety of blast load scenarios according to the scaled standoff distances, mainly considering the effects of wall thickness and boundary configuration, and obtained the dependence of the damage level of the wall on the blast impulse. Davidson et al. [16] studied nine different blast walls at different scaled standoffs, investigating the blast resistance of nine unidirectional restrained hollow concrete block (CMU) masonry walls of different configurations, including 6-inch-thick partially grouted CMU walls, 8-inch-thick partially grouted CMU walls, and 8-inch-thick partially grouted CMU walls with clay finish brick facings. It was shown that the ductility of the CMU walls became significantly improved after grouting and reinforcing. The clay brick facing outside the walls had a good energy absorption effect, which could reduce the deformation of the walls to some extent but usually produced outward-throwing debris in the blast. Keys and Clubley [17] conducted a study based on a large cross-sectional surge tube with a positive pressure duration of more than 100 ms. The dynamic response and brick dispersion pattern of a 10-sided masonry wall under a uniform blast surface load of more than 100 ms were investigated experimentally by Keys and Clubley [17].

Davidson et al. [4,5] investigated the effectiveness of SPUA in reinforcing plain CMU brick walls through comparative blast tests and further analyzed the typical failure mechanism of SPUA-retrofitted CMU walls, and examined the impact of window and door openings. The tests showed that the damage modes of SPUA-retrofitted CMU brick walls mainly included: (1) local fracturing of the wall caused by shock waves; (2) fragmentation of the block triggered by the direct action of shock waves; (3) shear tearing of SPUA near the support; (4) high pressure stresses generated by wall bending, leading to frontal crushing of the wall; (5) cracking at the mortar joint layer, leading to pulling and cracking of SPUA; and (6) bonding failure. As for walls with window and door openings, SPUA retrofitting still provides the same level of effective reinforcement but is significantly more prone to tearing at the openings and the corners. The effects of the SPUA method, support conditions, and blast load magnitude were also analyzed. The results showed that SPUA retrofitting was effective in improving the blast resistance of CMU walls, especially in reducing the generation of flying debris in the blast.

Baylot et al. [18] conducted blast tests on 1/4 scale down CMU walls and studied the damage patterns of walls without grouting, partial grouting, or complete grouting and FRP reinforcement, SPUA retrofitting, or steel bar reinforcement under various blast loadings to assess the risk level of flying debris. The results showed that SPUA retrofitting was effective in enhancing the integrity of the walls under blasts and preventing or reducing debris generation.

Johnson et al. [19] conducted blast tests of full-scale hollow CMU walls, as well as static and blast tests of 1/4 scale CMU walls to investigate the response of SPUA-retrofitted and SPUA-aramid fabric combined reinforced walls when blast loads or quasi-static surface loads were applied. The results showed that the reduced scale model was effective in simulating the response of walls under blast loading; both SPUA-retrofitted and SPUA-aramid fabric combined reinforcement can effectively reduce debris and significantly improve the stiffness and bending resistance of walls under static and dynamic tests. Additionally, the bending resistance of SPUA-retrofitted walls was improved by 1.9 to 4 times, and the bending resistance of SPUA-aramid fabric combined reinforced walls was improved by 5.5–7.5 times.

Irshidat et al. [20] investigated the blast resistance performance of reduced-scale model of SPUA-retrofitted and nanosheet-modified SPUA-retrofitted CMU walls by means of a surge tube apparatus. The SPUA-retrofitted walls were subjected to tensile damage at blast peaks up to 208.22 kPa; for the nanosheet-modified SPUA-retrofitted walls, horizontal shear damage occurred through the middle at the peak of 224.91 kPa. It should be noted that the blast simulator used in this test had a major limitation and cannot be used to study the fragmentation produced by the wall in real blast loading.

Wang et al. [13] conducted a blast test study of six-sided SPUA-retrofitted clay brick walls and autoclaved aerated concrete masonry walls to investigate the failure form of the reinforced walls under blast in order to compare the difference between single and double-sided SPUA retrofitting and the difference in blast-resistant performance between clay brick walls and autoclaved aerated concrete masonry walls commonly used in China. The test results showed that the polyurea coating can effectively reduce the splash debris produced in the explosion and ensure the integrity of the wall. The basic failure modes of autoclaved aerated concrete masonry walls and clay brick walls under blast loads were bending deformation and shear damage between mortar layers, respectively, due to the different material properties and adhesive failure modes of mortar and block. After SPUA retrofitting, the blast resistance of clay brick walls was improved by 4.5 to 11 times. The blast resistance of autoclaved aerated concrete masonry walls can be improved by about 15 times; the blast resistance of clay brick walls before and after reinforcement was much better than that of autoclaved aerated concrete masonry walls.

Wu et al. [21] carried out experimental studies on the blast resistance of unreinforced and SPUA-retrofitted masonry walls at scaled standoff values of 0.88, 0.584, and 0.35 kg/m^3, respectively. The results showed that the SPUA significantly improved the blast resistance of clay brick walls, that the SPUA-retrofitted walls could maintain their standing under a variety of blast, and that the reinforcement effect of SPUA on the rear surface was better than that of the front surface reinforcement.

Ji et al. [22] conducted a numerical simulation study and compared it with experiments on the dynamic response of SPUA-retrofitted masonry walls with a thickness of 240 mm under blast loading, analyzed the damage phenomena of brick masonry walls and SPUA-retrofitted brick walls under contact blast, and determined the damage response parameters of the walls. The results showed that the SPUA encapsulated the broken areas and debris of the wall within the SPUA-retrofitting layer, which had excellent blast performance. When the thickness of the SPUA layer increased to 8 mm, the breakage area of the masonry wall was reduced by 55.6% compared to that of the unreinforced one.

Yu et al. [23] conducted a field explosion test study of polymer-reinforced autoclaved aerated concrete (AAC) masonry walls of full size, with TNT explosive weights of 3000 kg and 10,000 kg and explosion distances of 70 m and 100 m. The test results showed that the shock wave arrival time predicted by CONWEP is accurate, and the difference in incident wave peak is within 30%. According to the post-blast damage final model, a three-stage damage assessment criterion for AAC masonry walls was established; the polymer coating on the wall surface significantly improved the blast resistance of the masonry walls.

However, due to the high cost, large dispersion, and limited effective data that can be captured in the blast tests, with the improvement of computer technology and computing efficiency, refined finite element (FE) simulation can efficiently compensate for the above deficiencies and provide the possibility to further accurately analyze the damage mechanism of SPUA-retrofitted masonry walls under blast loading. Davidson et al. [6,7] adopted LS-DYNA FE analysis software to compare and analyze different material models applicable to CMU blocks, and they concluded that the MAT_SOIL_AND_FOAM model could better simulate the mechanical properties of CMU blocks under blast loading. Furthermore, the effects of parameters such as elongation, thickness, initial modulus, yield strength of SPUA, and bond strength of wall-mortar-blocks were analyzed by FE simulation of SPUA-retrofitted hollow CMU walls. In addition, Hoemann et al. [24] further refined and supplemented the effects of boundary configurations of SPUA-retrofitted CMU walls mainly based on FE simulations. Irshidat et al. [20] performed FE analysis on their tests by ANSYS-AUTODYN and their model was able to more accurately predict the wall fragmentation velocity, centroid velocity, and damage pattern under blast. The results further demonstrated that both SPUA and nano-modified SPUA could significantly improve the blast resistance of the wall. Wang et al. [13,25] investigated the dynamic response of a clay brick wall under different charge, support reinforcement conditions, and polyurea materiality using the LS-DYNA program. The results showed that double-sided sprayed polyurea reinforcement can effectively improve the blast resistance of the wall. The increase in thickness of polyurea layer on the front surface significantly improves the blast resistance of the wall, while the effect of SPUA layer thickness on the back surface is relatively small; the increase in modulus of elasticity of polyurea material can effectively enhance the blast resistance of the wall, but its density has a negative impact.

In this paper, based on the three far-range blast tests conducted by Davidson et al. [4,5] and using the commercial FE analysis software LS-DYNA [26], a FE model of the SPUA-retrofitted CMU masonry wall under the action of far-range blast was established and compared with the test results for verification. The effects of SPUA layer thickness, boundary anchorage method, and anchorage length on the blast resistance performance of masonry walls were further discussed in order to provide a more in-depth reference for further engineering design and analysis.

2. Blast Test and FE Modeling

2.1. Existing Blast Test

Davidson et al. [4,5] carried out blast tests of SPUA-retrofitted hollow CMU masonry infill walls [4]; the mechanical properties of the materials are shown in Figure 1. The test is divided into three blast loading scenarios, and Figure 2 provides the test setups in each shot, where the wall is 3660 mm in height, 2240 mm in width, and 200 mm in thickness, with the CMU block size is approximately 400 mm × 200 mm × 200 mm. Two walls were tested simultaneously in each shot, and the upper and lower ends of the wall were fixed in a reusable reinforced concrete frame by angle steel and steel plates to ensure that the wall was under unidirectional force. The dynamic response and damage patterns of the SPUA-retrofitted CMU walls were evaluated for different blast load levels by varying the explosive charge and blast distance in the three tests. Due to the difficulty in obtaining the data in the blast test, complete data were obtained only for some of the sensors. The data obtained from the measurements are given in Table 1.

Although Davidson et al. [4,5] performed a series of subsequent FE simulations of the above tests [7] and were able to obtain a better overall response of the wall, only partial load scenarios were simulated. Due to the limitation of the computing efficiency at that time, a simplified model was used which failed to reproduce the damage pattern of the full-size wall as well as the local damage, especially the blocking effect of the SPUA retrofitting on the wall fragments under larger blast loads.

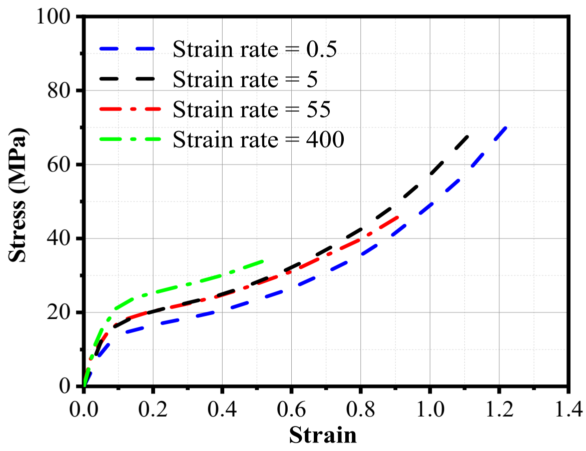

Figure 1. Stress-strain curves of SPUA at different strain rates.

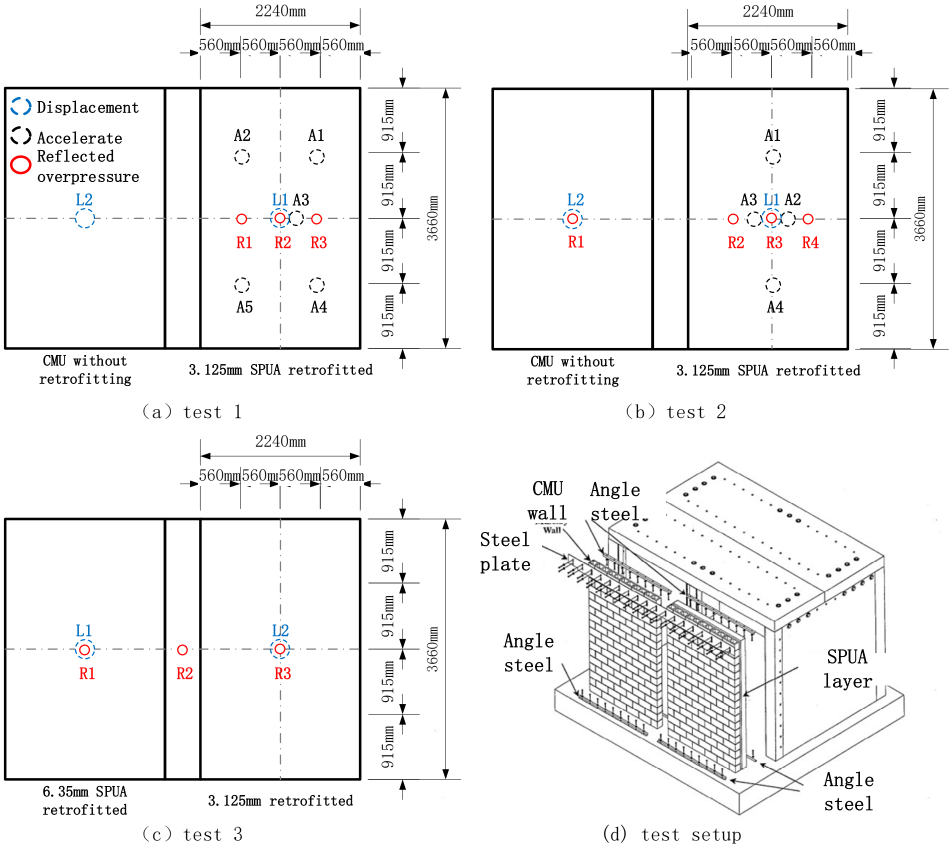

Figure 2. Test setups.

Table 1. Main test data.

Sensor ID	R1 (MPa)	R2 (MPa)	R3 (MPa)	L1 (mm)	L2 (mm)
Test 1	0.393	0.362	0.303	184	Collapse
Test 2	1.096	1.324	1.200	Collapse	Collapse
Test 3	0.409	0.479	0.447	238	198

2.2. Material Models and Parameters

Taking the double-layer SPUA-retrofitting model as an example, Figure 3 shows in detail the process of building the FE model of the wall and how the refined mesh is divided. The wall FE model used in the numerical simulation process is still a refined separated model with a mesh size of 30 mm. The mortar and block and steel frame fabrication at the upper and lower ends of the wall were modeled with 8-node hexahedral solid cells, with two layer of mortar mesh. Due to the thin thickness of the SPUA-retrofitting layer in the test, shell cells were used for modeling, and the mesh size was kept consistent with the wall mesh size division.

The main control parameters in the tiebreak contact are axial failure stress (NFLS) and shear failure stress (SFLS), respectively. The NFLS and SFLS were set at 0.3 MPa accordingly; in addition, the static friction coefficient (FS) was set at 0.8 and the dynamic friction coefficient (FD) was set at 0.6 [27]. Since the SPUA layer usually has a good bond with the wall, the tiebreak type contact was also set between the SPUA layer and the wall, and the NFLS and SFLS were set at 0.7 MPa and 1.7 MPa, respectively. The *AUTOMATIC_SURFACE_TO_SURFACE contact was used between the SPUA-retrofitted wall and the supports to simulate the boundary restraint effect. In addition, since the SPUA retrofitting had a long anchorage length at the boundary in the test, the top and bottom ends of SPUA can be considered as fixed ends, which is achieved by setting the *BOUNDARY_SPC_SET card.

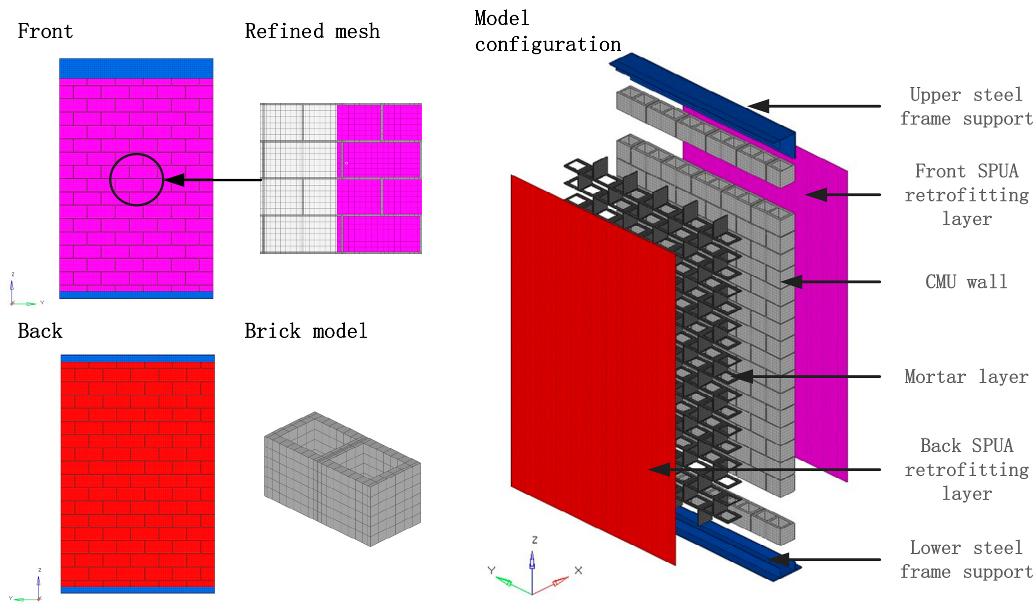

Figure 3. FE Model.

The blocks used in the tests were hollow CMU blocks, and Davidson et al. [7] compared a variety of material models and concluded that the best results were obtained using No. 5 MAT_SOIL_AND_FOAM material to simulate CMU blocks. The mortar was concrete mortar, using the No. 96 MAT_BRITTLE_DAMAGE model with a strength grade of M5 and an average compressive strength of 5.0 MPa. Empirical equations for E_b (elastic modulus of block) and E_m (elastic modulus of mortar) were fitted based on a large amount of test data by literature [28] as shown in Equations (1) and (2), respectively, where f_1 is the average compressive strength of block and f_2 is the average compressive strength of mortar. The values of the main material model parameters in the numerical model are given in Tables 2 and 3.

$$E_b = 4467 f_1^{0.22} \quad (1)$$

$$E_m = 1057 f_2^{0.84} \quad (2)$$

Table 2. CMU block material model parameters.

Density (kg/m^3)	Shear Modulus (MPa)	Bulk Modulus (MPa)	A_0	A_1	A_2	Tensile Strength (MPa)
1900	5433	41,368	0.616	0	0	1.38

Table 3. Parameters of mortar material model.

Density (kg/m^3)	Young's Modulus (MPa)	Poisson's Ratio	Ultimate Compression Strength (MPa)	Ultimate Shear Strength (MPa)	Fracture Toughness (N/m)	Shear Retention Rate	Bulk Viscosity (MPa/s)	Compression Strength (MPa)
1800	4016	0.21	0.55	0.95	140	0.03	0.72	4.9

As for the hollow CMU blocks, it has been shown that the soil and foam model of MAT_5 can better characterize their mechanical properties under blast loading [18] with the parameters shown in the following table.

For the selection of material card for polyurea, the MAT_PIECEWISE_LINEAR_PLATICITY material model No. 24 was used to better simulate the response of polyurea reinforcement under blast loading. The material card No. 24 is a multi-linear elasto-plastic material model, which can consider the response of different strain rates on the material by inputting the stress-strain curves at different strain rates effects. The main parameters of the polyurea material in the model are given in Table 4. In addition, the stress-strain curves of polyurea at different strain rates in Figure 1 need to be entered through the *DEFINE_TABLE and *DEFINE_CURVE cards.

Table 4. Parameters of SPUA.

Density (kg/m^3)	Young's Modulus (MPa)	Poisson's Ratio	Ultimate Tensile Strength (MPa)	Cutline Modulus (MPa)	Failure Coefficient
1440	234.4	0.3	9.65	23.44	0.8

Since the dynamic response and damage pattern of the wall were mainly considered in this simulation, and the external frame of the wall did not show obvious damage in the test, based on the calculation efficiency, the MAT_RIGID model was used; its rotation and displacement in any direction are restricted. At the same time, in order to better simulate the damage pattern of the wall under the blast load and to prevent unit distortion, the *MAT_ADD_EROSION keyword was added to the mortar and block models, and it was determined through trial calculations that the results were optimal when the maximum principal strain term MXEPS was used as the failure criterion for the unit, with a value of 0.01.

The parameters of the blast load were not given in the original test, but the reflected overpressure curves for multiple points on the wall measured in each test round were given. In analyzing the test data given in Table 1, it can be assumed that the blast load acting on the wall was relatively uniform in each test, which can be simplified to a uniform load by applying the *LOAD_SEGMENT _SET card on the blast surface of the wall. The overpressure curves to be entered in the simulation of the three tests were obtained by averaging the overpressure curves measured in each test, as shown in Figure 4. The peak value for load 1 was 0.353 MPa, the peak value for load 2 was 1.207 MPa, and the peak value for load 3 was 0.445 MPa.

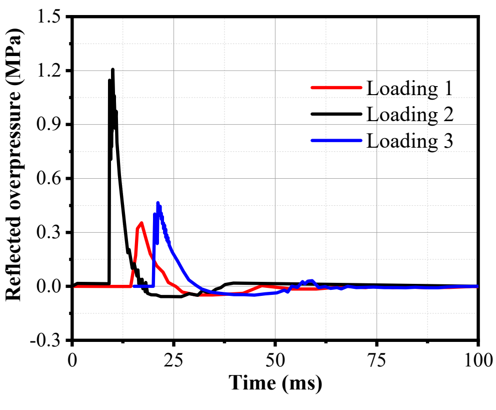

Figure 4. Stress-strain curves of SPUA at different strain rates.

3. Comparison and Analyses

In this section, based on the blast test data from AFRL, the finite element model described in the previous section is used to simulate the tests with different blast load conditions for three rounds. The accuracy of the finite element model in simulating the overall dynamic response of the wall under blast load is analyzed, and the effectiveness of the finite element method in simulating the damage pattern of the wall under blast load as well as the local damage is focused on.

3.1. Comparison with the Test Results

There were two hollow CMU masonry infill walls in Test 1: one with a 3.175 mm polyurea reinforcement layer sprayed on the inside of the wall and one without any reinforcement. The peak overpressure of the blast load on the wall in Test 1 was the smallest in the three-shot test.

The velocity and displacement time curves of the wall at different measurement points in Test 1 obtained from the test and numerical simulation are shown in Figure 5. It was found that the numerical method agreed well with the time course curves obtained from the test, and the errors of the peak displacement time course obtained from the simulation compared to the test results were 2.7% and 7.7% at point L1 and A1 of the polyurea reinforced wall, respectively. However, the simulations for the rebound phase of the wall generally had relatively large errors. For the simulation results of the unreinforced wall at point L2, the velocity time course curves can be fitted well with the experimental data, and the velocities eventually converged to about 2 m/s, indicating that the wall had lost resistance under the blast load. It should be noted that for the displacement time curve at the midpoint (L2) of the unreinforced CMU wall, no valid data were obtained in the test due to severe deformation. The simulation results show that the displacement time curve at the midpoint of the unreinforced CMU wall did not rebound under Load 1, but exceeded 500 mm at 150 ms, and the wall eventually collapsed.

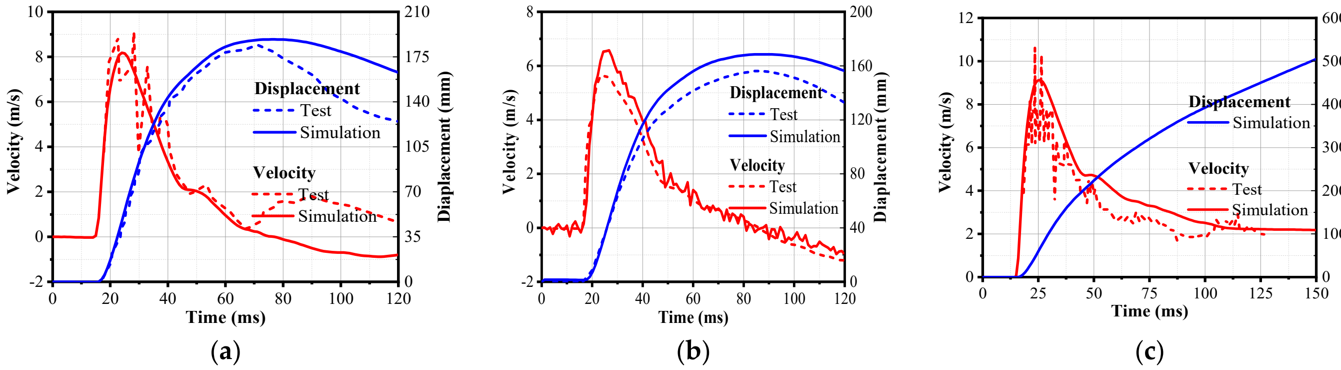

Figure 5. Velocity- and displacement-time histories in Test 1 at measuring point: (**a**) L1; (**b**) A1; (**c**) L2.

Figure 6 further shows the displacement clouds of the hollow CMU masonry infill wall before and after the sprayed polyurea reinforcement. It was found that due to the presence of polyurea reinforcement, the resistance of the wall gained a great increase, the maximum deflection of the wall under the blast load decreased, and finally the overall rebound occurred. It follows that the deformation of the unreinforced CMU masonry infill will increase throughout the dynamic response and will eventually collapse under the action of gravity, etc.

Figure 7 shows the local damage of the wall obtained in the test and simulation under Load 1. The polyurea reinforced hollow CMU masonry infill wall in the test produced local damage concentrated at the upper and lower ends of the wall. Similar results were obtained in the numerical simulation, where the blocks at the end of the wall appeared to be broken, and the shear strains in the wall obtained from the simulation were also concentrated at the upper and lower ends of the wall. It shows that the presence of polyurea reinforcement layer increases the overall resistance of the wall while also leading to stress-strain concentration at the end of the wall, which results in local damage destruction. In Test 2, the charge volume and charge distance were 2 and 0.86 times that of Test 1, respectively, which produced the largest peak reflected overpressure, and the average value of the peak measured at several reflected overpressure measurement points on the wall in the test reached 1.207 MPa. Two hollow CMU masonry infill walls were tested at the same time: one side was reinforced with 3.175 mm polyurea sprayed on the inner side and the other side was without any reinforcement. Both walls eventually collapsed completely in the test and limited test data were obtained due to the excessive blast load.

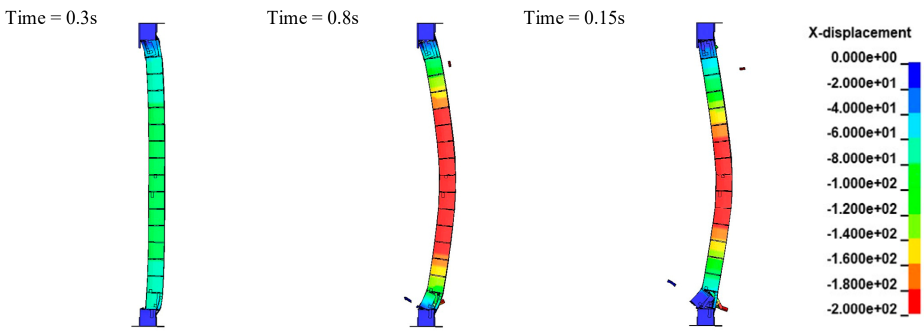

(**a**)

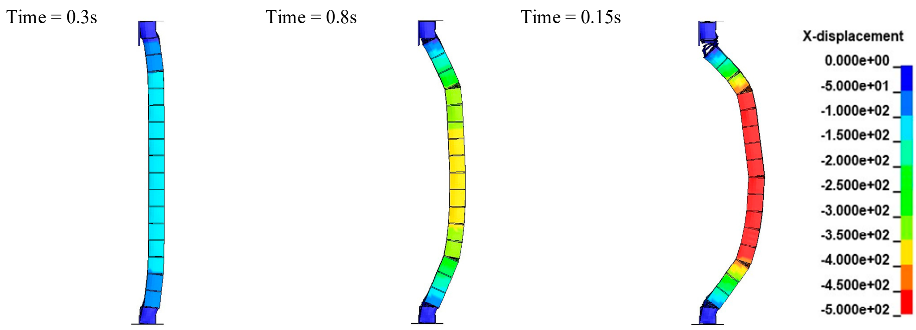

(**b**)

Figure 6. Dynamic responses of the wall in Test 1: (**a**) retrofitted with SPUA of 3.175 mm; (**b**) No retrofitting.

(**a**) (**b**) (**c**)

Figure 7. Damage of SPUA-retrofitted wall: (**a**) local damage; (**b**) simulated damage; (**c**) shear stress distribution.

Figure 8 shows the velocity and displacement time curves of the hollow CMU masonry infill wall at the midpoint of the wall before and after reinforcement through finite element simulation. The velocity at the midpoint of the wall reached a maximum of approximately 22.6 m/s without reinforcement with polyurea and kept splashing at this high speed. The peak velocity at the midpoint of the wall decreased to 16.2 m/s after reinforcement with the 3.175 mm polyurea layer, which was reduced by 28.3%, and the velocity continued to decrease due to the restraining effect of the polyurea reinforcement layer, and the velocity decreased to about 5.5 m/s at 0.2 s. Although the midpoint displacement time course curve of the CMU wall continued to diverge before and after reinforcement, the wall eventually collapsed. The midpoint dispersion distance at 0.2 s after reinforcement was approximately 2.0 m, which is only 46.4% of the midpoint dispersion distance of the unreinforced wall.

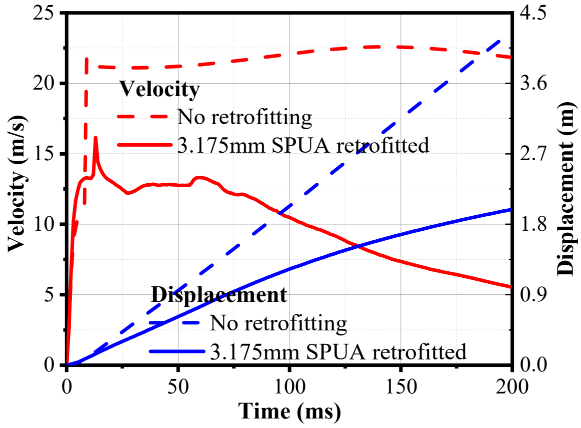

Figure 8. Velocity- and displacement-time histories in Test 2.

Figure 9 shows the damage pattern of the hollow CMU masonry infill wall at around 0.2 s obtained from numerical simulations before and after reinforcement with sprayed polyurea. It was found that the blocks in the wall completely broke up and flew apart under the blast load, and the wall eventually collapsed, regardless of whether polyurea reinforcement was applied or not. However, the back side of the polyurea-reinforced hollow CMU masonry infill wall retained a high degree of integrity due to the polyurea layer, and most of the fragments generated in the explosion were stopped by the polyurea layer. In contrast, without the polyurea reinforcement, the wall completely shattered under the blast load, forming a large number of fine fragments that were thrown outward, posing a great safety threat. This shows that the polyurea reinforcement of 3.175 mm served as an excellent protection against flying debris under Load 2, which reached a peak of 1.207 MPa although could not prevent the collapse of the wall. Test 3 was designed to evaluate the difference brought by different forms of polyurea reinforcement on the wall's blast resistance performance improvement. Two polyurea-reinforced hollow CMU masonry infill walls were tested simultaneously: one with 6.35 mm polyurea reinforcement on the back side and the other one with 3.175 mm polyurea reinforcement on both sides. The load in Test 3 was higher than in Test 1 but less than in Test 2. The charge volume and charge distance were 2 and 1.3 times that of Test 1, respectively, and the average value of the peak value measured at several reflective overpressure measurement points on the wall was 0.445 MPa, which increased by 26% compared to Load 1.

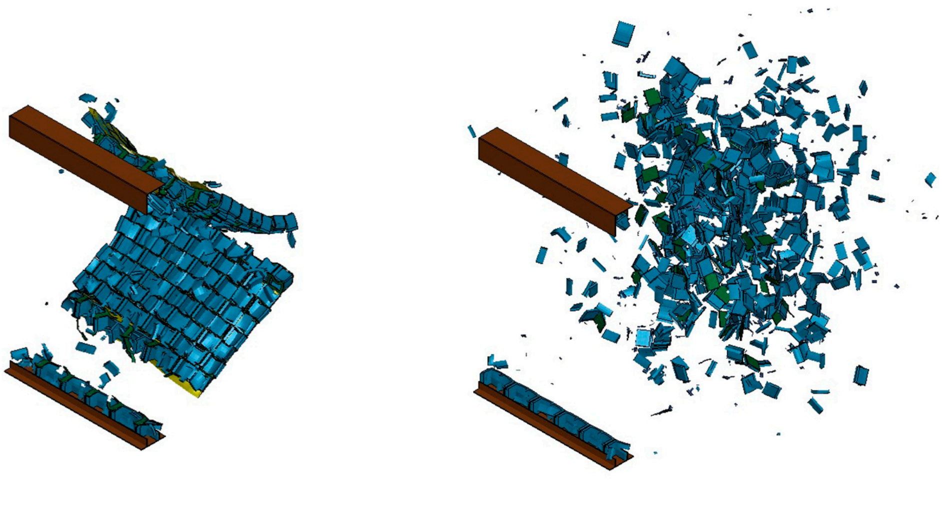

(**a**) (**b**)

Figure 9. Comparison of damage pattern in Test 2: (**a**) 3.175 mm SPUA-retrofitted; (**b**) No retrofitting.

The differences in the velocity and displacement time profiles of the wall midpoints for the two different forms of reinforcement are shown in Figure 10; the two forms were supplemented by the velocity and displacement time profiles of the midpoints of the unreinforced hollow CMU masonry-filled walls obtained from the simulation under Load 3. Under Load 3, the peak displacement of the midpoint of the wall obtained from the simulation was large relative to the test results, with peak deflection errors of 8.8% and 11.6% for the single- and double-sided reinforcement cases, respectively. It is easy to see from the simulation results that the peak deflection at the midpoint of the wall was reduced by 14.7% in the form of double-sided reinforcement with the same thickness of the reinforcement layer, while the resilience of the wall was enhanced. It shows that the sprayed polyurea double-sided reinforcement can more effectively improve the blast resistance of the wall. The velocity and displacement time curves at the midpoint of the unreinforced CMU wall under Load 3 indicate that the wall will eventually collapse, with the velocity eventually converging at about 5.0 m/s and the displacement already exceeding 873 mm at 0.15 s.

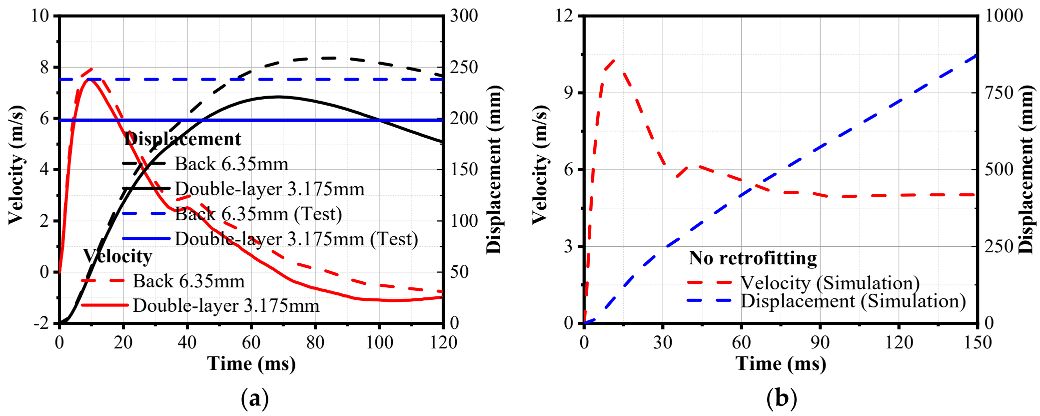

Figure 10. Velocity- and displacement-time histories in Test 2: (**a**) retrofitted; (**b**) no retrofitting.

Figure 11 compares the final damage pattern and local damage of the wall in the test and simulation. The experimental results are similar to the simulated results, where the wall as a whole underwent bending damage, concentrated on the end blocks of the wall to produce fragmentation. Moreover, the bond between the polyurea reinforcement layer and the wall at the front of the wall separated at the top when the double-sided polyurea reinforcement was used.

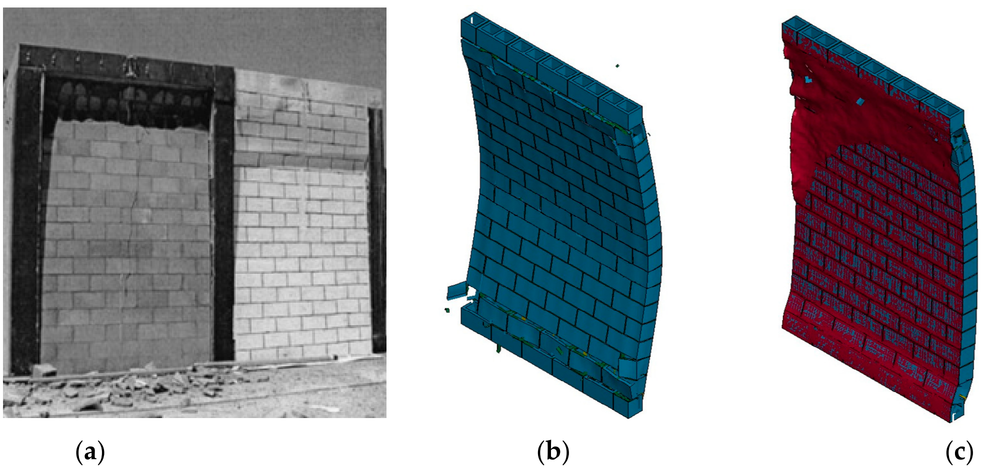

Figure 11. Damage of SPUA-retrofitted wall: (**a**) test results; (**b**) 6.35 mm SPUA-retrofitted; (**c**) double-layer 3.125 mm SPUA-retrofitted.

3.2. Error Analysiss

In summary, the finite element method effectively simulates the rupture and splash of debris occurring in hollow CMU masonry infill walls under higher blast loads, which complements the verification of the preventive effect of polyurea material against wall splash debris under blast loads. In addition, the numerical simulation results also show that when double-sided polyurea reinforcement is used, it can improve the blast resistance of the wall more effectively compared to single-sided reinforcement with the same total thickness of the reinforcement layer; however, the effect is relatively limited.

Taken together, the results show that the finite element method can effectively simulate the overall dynamic response and damage morphology of polyurea-reinforced hollow CMU masonry infill walls under blast loading, as well as the damage that occurs locally. The simulation results also effectively complement the data results that are difficult to obtain in blast tests, further demonstrating the effectiveness of sprayed polyurea reinforcement in enhancing the blast resistance of walls.

However, there are still some deviations between the above simulation results and the test results. The comparative test and simulation data are presented in Table 5, and the simulation results are generally large compared to the test results. At the same time, there is still a gap between the simulation of local damage and the actual situation in the test. On the one hand, this is due to more chance factors in the explosion test, key explosion load data not provided in the literature, and the simulation using a simplified approach of explosion load application. On the other hand, the study of mechanical properties of block and polyurea materials still needs further examination and improvement.

Table 5. Experimental and numerical results under different scenarios.

Test	Retrofitting Thickness (mm)	Center Displacement (mm)		Description
		Test	Simulation	
Test 1	0 3.175	Collapse 184	Collapse 189 (+2.7%)	Collapse. Mortar cracking, end brick broken.
Test 2	0 3.175	Collapse Collapse	Collapse Collapse	Completely damaged. Damages without fragments.
Test 3	6.5 3.175 (double-layer)	238 198	259 (+8.8%) 211 (+11.6%)	Mortar cracking, end brick broken. SPUA separating at the front.

4. Parametric Analyses

In this section, the effects of polyurea reinforcement layer boundary conditions, SPUA-retrofitting layer thickness, and anchorage length on the wall blast resistance enhancement will be further discussed based on the previously discussed finite element model, and the blast resistance performance of SPUA-retrofitted and grouted CMU walls will also be compared and analyzed.

4.1. Boundary Constraint at the SPUA Layer

Boundary conditions usually have a large impact on the overall dynamic response of the structure, and this section will discuss the effect of different polyurea reinforcement layer boundary conditions on the blast resistance performance improvement of the wall when reinforcing an existing wall.

The analysis is mainly based on the back side 3.175 mm SPUA-retrofitted CMU masonry infill walls. The effects of two different restraint conditions, four-sided restraint, and upper and lower end restraint of the polyurea reinforcement layer, on the overall dynamic response of the wall and damage under three different loading conditions were considered.

Figure 12 compares the displacement time curves of the polyurea layer reinforced hollow CMU masonry infill walls with different boundary conditions under three different loadings. Under the action of Load 1 and Load 3 with smaller peak load, the peak displacement at the midpoint of the wall was reduced by 2.6% and 12.4%, respectively, by restraining the four sides of the polyurea reinforcement layer, which had a relatively small effect, but the rebound capability of the wall was significantly improved in the rebound phase. Under the action of Load 2 with a greater peak, regardless of which reinforcement boundary was adopted for the polyurea reinforcement layer, the displacement time curve of the wall eventually diverged due to the failure of the boundary restraint at the early stage of the dynamic response of the wall, which is less influenced by different forms of restraint.

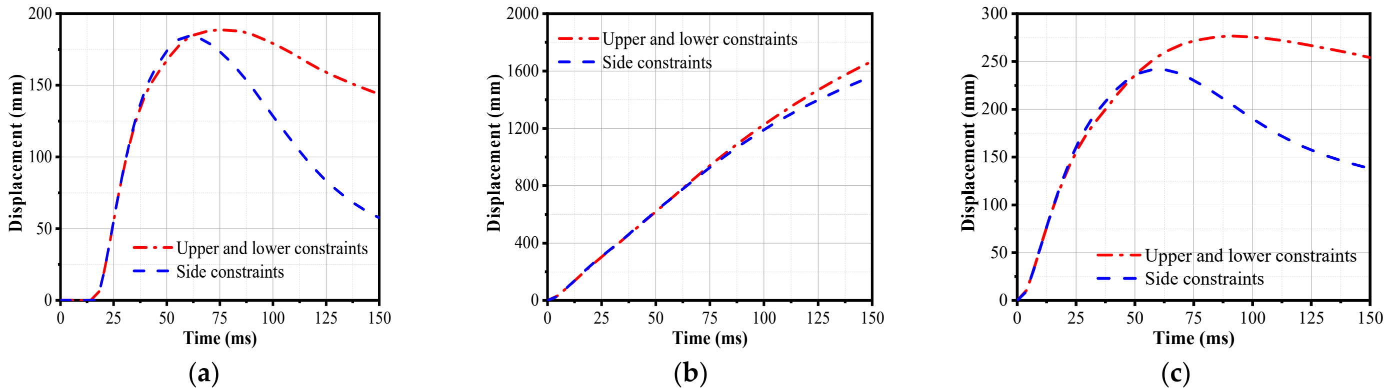

Figure 12. Influence of boundary constraints at the SPUA layer to wall center displacement-time histories under different loadings: (**a**) Load 1; (**b**) Load 2; (**c**) Load 3.

The damage morphology of the four-sided constrained CMU walls with a SPUA-retrofitted layer is shown in Figure 13, where the right side in each image is the back side, blue is the CMU masonry infill wall, and yellow is the SPUA-retrofit layer. It can be seen that under Load 1, although the resilience of the wall was increased after the four-sided restraint of the polyurea reinforcement layer, the increase in the restraint of the polyurea layer increases the binding force on the four sides of the wall, resulting in more severe fragmentation of the blocks at the left and right ends of the wall. Under the action of Load 2 with greater peak overpressure, as the SPUA-retrofitting layer is prone to tearing at the boundary, not only does the boundary construction of the SPUA-retrofitting layer with four fixed sides have relatively little effect on the overall dynamic response of the wall, but in examining the damage pattern, the increase in the tearing of the SPUA-retrofitting layer reduces its integrity and protective ability against splash debris. Therefore, the boundary constraint of the enhanced polyurea reinforcement layer usually has a limited effect on the improvement of the blast resistance of the wall, while there is a side effect of increasing the local damage of the wall.

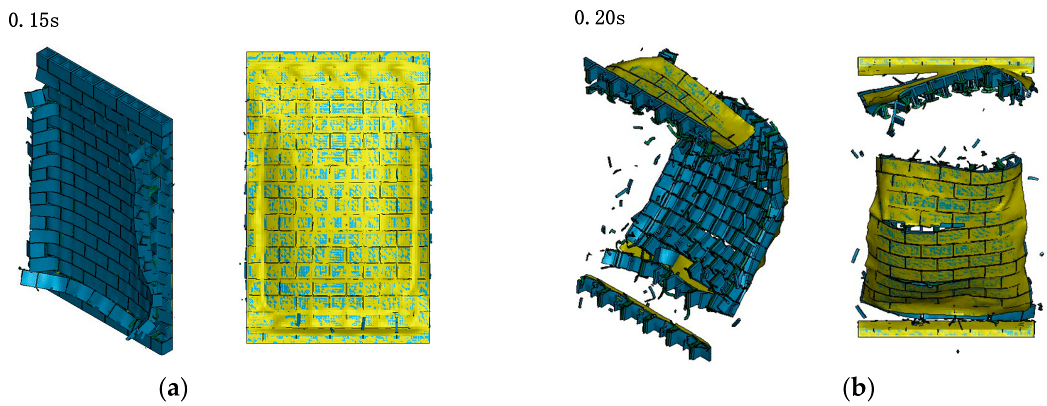

Figure 13. Influence of boundary constraints at the SPUA layer to damage pattern under different loadings: (**a**) Load 1; (**b**) Load 2.

4.2. Thickness of SPUA Layer

This section further investigates the effect of SPUA-retrofitting layer thickness on the blast resistance performance of CMU masonry infill walls. The main comparative analysis is of the differences in the blast resistance performance of hollow CMU masonry infill walls reinforced with 3.175 mm, 6.35 mm, and 12.7 mm polyurea on the back, respectively, under three different loading conditions, i.e., Load 1, Load 2, and Load 3.

The displacement time curves at the midpoint of the hollow CMU masonry infill wall reinforced with different thicknesses of polyurea layers under three different loads are shown in Figure 14. As the thickness of the SPUA-retrofitting layer increased, the peak displacement at the midpoint of the wall decreased subsequently, and at the same time the resilient energy of the wall was enhanced. Under Load 1, the peak midpoint displacement of the wall decreased by 3.2% and 10.1% with an increase of SPUA thickness from 3.175 mm to 6.35 mm and 12.7 mm, respectively. The peak midpoint displacement of the wall decreased by 6.2% and 13.8%, respectively, when the load was increased to Load 3. At Load 2, the dynamic response type of the wall changed when the polyurea thickness increased to 12.7 mm, and the midpoint displacement of the wall no longer diverged and produced a significant rebound.

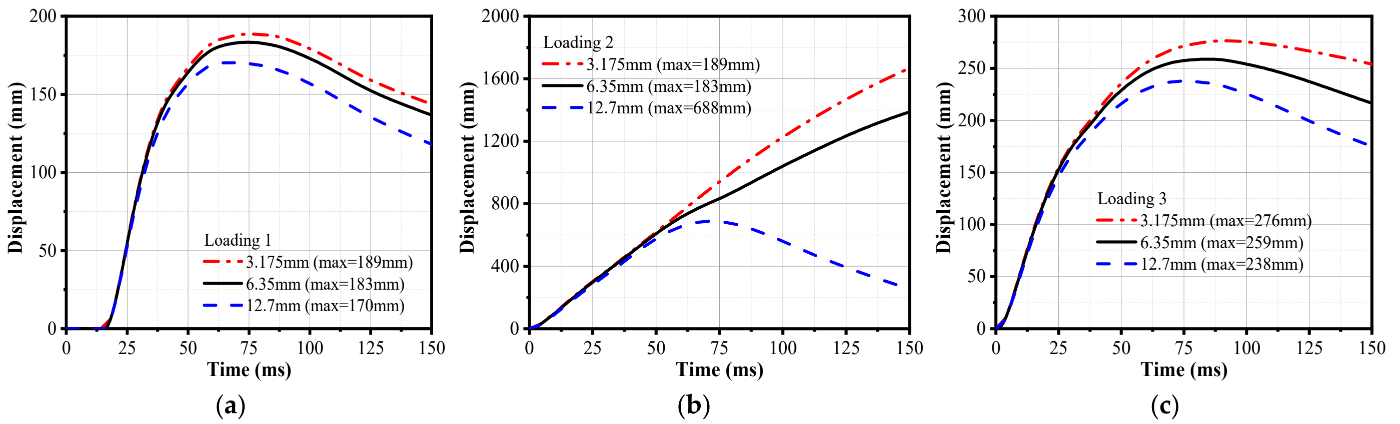

Figure 14. Influence of SPUA layer thickness to wall center displacement-time histories under different loadings: (**a**) Load 1; (**b**) Load 2; (**c**) Load 3.

Figure 15 shows a comparison of the effect of three different SPUA-retrofitting thicknesses on the final damage pattern of the wall under the action of Load 2 with the maximum peak blast overpressure. The magnitude of improvement in the blast resistance performance of the wall brought about by the change in the thickness of the SPUA-retrofitting layer was significant as the load increased. When the thickness of the SPUA-retrofitting layer was increased to 6.35 mm, tearing occurred only at the end of the SPUA layer. When the thickness of the SPUA-retrofitting layer was further increased to 12.7 mm, no tearing occurred, and the final damage pattern of the wall was changed. Although the blocks in the wall were all broken due to the blast overpressure, the wall rebounded significantly and retained a better overall integrity due to the SPUA-retrofitting layer. This indicates that at that time, the resistance of the wall was almost completely provided by the SPUA retrofitting.

In summary, the enhancement of the blast resistance performance of the wall by the thickness of the SPUA-retrofitting layer increases with the increase of the blast load acting on the wall. When the blast load is small, the improvement of the blast resistance of the wall is relatively limited, but as the blast load increases, especially under extreme loads, the SPUA-retrofitting layer provides the main resistance, which ultimately determines the final damage pattern of the wall.

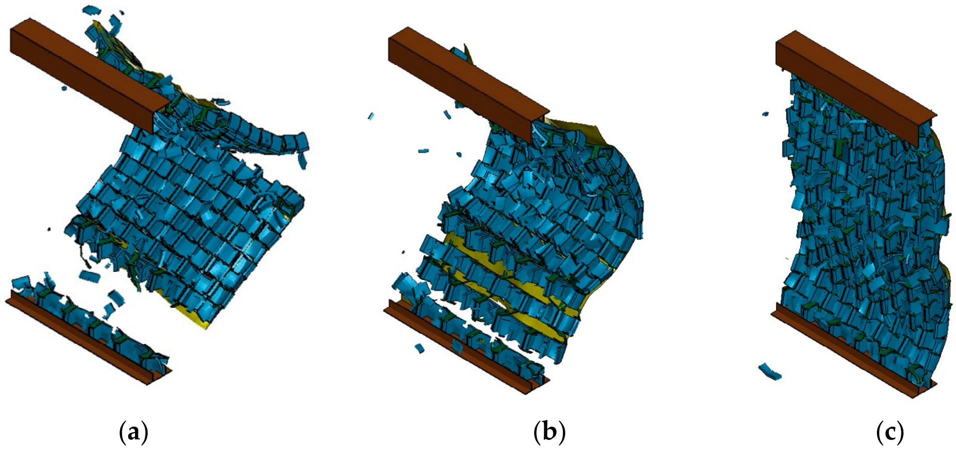

Figure 15. Influence of SPUA layer thickness to damage pattern: (**a**) 3.175 mm; (**b**) 6.35 mm; (**c**) 12.7 mm.

4.3. Anchorage Length of SPUA Layer

As shown in Figure 16, when polyurea is used for wall reinforcement in practical applications, the SPUA layer is usually extended for a distance to the floor and ceiling and anchored with angles and rivets. In this section, the effect of different anchorage lengths of SPUA-retrofitting layers on the blast resistance performance of the reinforced walls is analyzed using FE simulation.

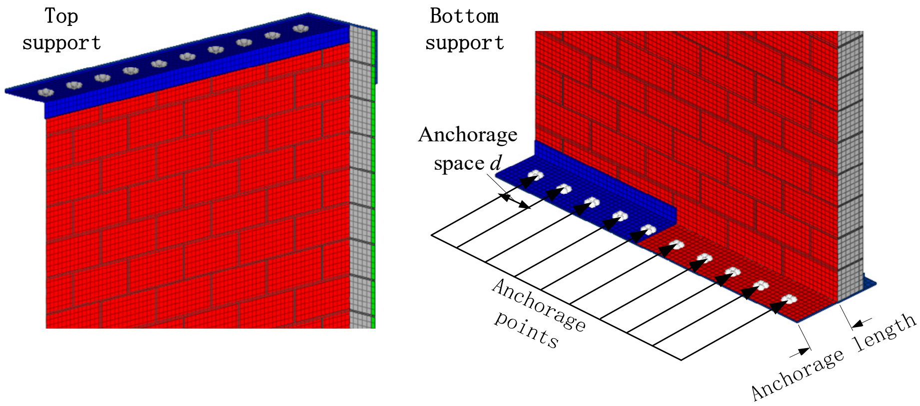

Figure 16. Anchorage of SPUA layer.

The displacement time-histories at the center of the SPUA-retrofitted CMU masonry infill wall under different levels of blast loads with the anchorage lengths of 15 cm, 30 cm, and 40 cm are shown in Figure 17, respectively. The time course curves of displacement at the wall center overlap with the maximum displacement peak error less than 1.2% under different anchorage lengths, and no failure of the bearing was seen in each scenario. It can be surmised that the anchoring length of the SPUA layer in the bearing does not have a significant effect on the overall response of the reinforced wall. In conclusion, a high accuracy can be obtained by using simplified boundary conditions when analyzing the blast resistance of SPUA-retrofitted walls using the FE method. Meanwhile, in practical engineering applications, the current polyurea anchoring method can provide sufficient binding force, and the anchoring length of the SPUA-retrofitting layer can meet the structural requirements.

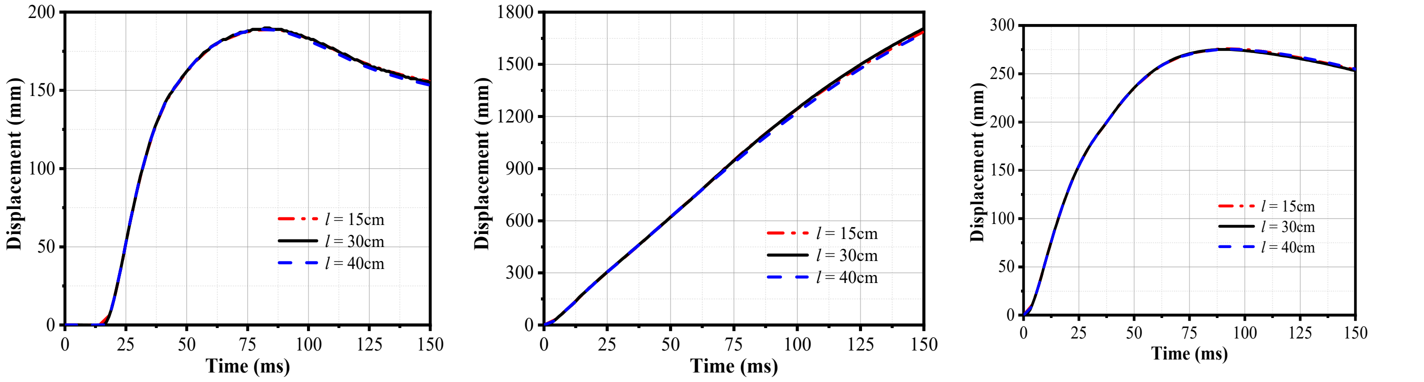

Figure 17. Influence of anchorage length to wall center displacement-time histories: (**a**) Load 1; (**b**) Load 2; (**c**) Load 3.

5. Conclusions

In this paper, a numerical simulation study was carried out based on three sets of full-scale blast tests of SPUA-retrofitted hollow CMU masonry infill walls. Firstly, based on the existing test data, the effectiveness of the finite element method in simulating the overall dynamic response, damage morphology, and local damage of SPUA-retrofitted hollow CMU masonry infill walls under the blast load was further verified. Further parametric sensitivity analyses were also carried out to investigate the effect of boundary conditions and thickness of a SPUA-retrofitting layer on the blast-resistant performance of the wall and also to compare the difference in blast-resistant performance between SPUA-retrofitted and grouted CMU masonry infill walls. The main conclusions are:

(1) The FE simulation results can fit well with the experimental results, and the overall and local damage of the polyurea-reinforced CMU masonry infill wall under the blast load can be simulated better;
(2) Increasing the boundary constraints of the polyurea reinforcement layer has limited improvement on the blast resistance of the wall, although it tends to aggravate local damage such as block fragmentation and polyurea tearing. In addition, the effect of the anchorage length of the polyurea reinforcement layer on the dynamic response of the wall is very small;
(3) When the load is small, the thickness of the SPUA-retrofitting layer has less influence on the blast resistance performance of the masonry infill wall. As the blast load increases, increasing the thickness of the SPUA-retrofitting layer can effectively enhance the blast resistance performance of the wall and determine the final damage pattern of the wall;
(4) Compared with grouted CMU masonry infill walls, SPUA-retrofitting CMU masonry infill walls exhibit better blast resistance performance.

Author Contributions: Conceptualization, Y.Z.; writing—original draft, J.H.; investigation, W.Z.; resources, W.Z.; writing—review and editing, F.H.; formal analysis, X.Y.; supervision, Y.Z. All authors have read and agreed to the published version of the manuscript.

Funding: This research was funded by National Natural Science Foundation of China grant number 12102476.

Conflicts of Interest: The authors declare no conflict of interest.

References

1. Ettouney, M.; DiMaggio, P.; Hapij, A. Analysis of masonry bearing walls to blast threats. In Proceedings of the Structures Congress, ASCE, San Diego, CA, USA, 19–21 October 2003.
2. Johnson, C.F. *Concrete Masonry Wall Retrofit Systems for Blast Protection*; Texas A&M University: College Station, TX, USA, 2013.

3. Konx, K.J.; Hammons, M.I.; Lewis, T.T. *Polymer Materials for Structural Retrofit*; Force Protection Branch, Air Expeditionary Forces Technology Division, Air Force Research Laboratory: Force Base, OH, USA, 2000.
4. Davidson, J.S.; Porter, J.R.; Dinan, R.J.; Hammons, M.I.; Connell, J.D. Explosive testing of polymer retrofit masonry walls. *J. Perform. Constr. Facil.* **2004**, *18*, 100–106. [CrossRef]
5. Davidson, J.S.; Fisher, J.W.; Hammons, M.I.; Porter, J.R.; Dinan, R.J. Failure mechanisms of polymer-reinforced concrete masonry walls subjected to blast. *Struct. Eng.* **2005**, *131*, 1194–1205. [CrossRef]
6. Davidson, J.S.; Moradi, L.; Dinan, R.J. *Selection of a Material Model for Simulating Concrete Masonry Walls Subjected to Blast*; DTIC: Fort Belvoir, VA, USA, 2004.
7. Davidson, J.S.; Sudame, S.; Dinan, R.J. *Development of Computational Models and Input Sensitivity Study of polymer Reinforced Concrete Masonry Walls Subjected to Blast*; DTIC: Fort Belvoir, VA, USA, 2004.
8. Ackland, K.; St John, N. *Experimental and Numerical Investigations into Polymeric Coatings for Blast Protection*; Defense Science and Technology Organization Victoria (Australia) Maritime Platforms Division: Canberra, Australia, 2011.
9. Ciornei, L. *Performance of Polyurea Retrofitted Unreinforced Concrete Masonry Walls under Blast Loading*; University of Ottawa: Ottawa, ON, Canada, 2012.
10. Abou Zeid, B.M.K. *Experimental and Analytical Strategies to Assess and Improve the Dynamic Response of Unreinforced Concrete Masonry Walls under Blast Loading*; McMaster University: Hamilton, ON, Canada, 2010.
11. Michaloudis, G.; Gebbeken, N. Modeling masonry walls under far-field and contact detonations. *Int. J. Impact Eng.* **2019**, *123*, 84–97. [CrossRef]
12. Pu, X.F. Numerical Analysis on Responses of Elastomer-Reinforced Concrete Masonry Walls Subjected to Blast. Master's Thesis, Ningbo University, Ningbo, China, 2009.
13. Wang, J.; Ren, H.; Wu, X.; Cai, C. Blast response of polymer-retrofitted masonry unit walls. *Compos. Part B Eng.* **2017**, *128*, 174–181. [CrossRef]
14. Li, Z.; Chen, L.; Fang, Q.; Chen, W.; Hao, H.; Zhang, Y. Experimental and numerical study of basalt fiber reinforced polymer strip strengthened autoclaved aerated concrete masonry walls under vented gas explosions. *Eng. Struct.* **2017**, *152*, 901–919. [CrossRef]
15. American Society of Mechanical Engineers. Damage to brick masonry panel walls under high explosive detonations. In Proceedings of the Pressure Vessels and Piping Conference, Orlando, FL, USA, 27–31 July 1997; Volume 351, pp. 207–216.
16. Davidson, J.S.; Hoemann, J.M.; Shull, J.S.; Salim, H.A. *Full-Scale Experimental Evaluation of Partially Grouted Minimally Reinforced Concrete Masonry Unit (CMU) Walls against Blast Demands*; DTIC: Fort Belvoir, VA, USA, 2011.
17. Keys, R.A.; Clubley, S.K. Experimental analysis of debris distribution of masonry panels subjected to long duration blast loading. *Eng. Struct.* **2017**, *130*, 229–241. [CrossRef]
18. Baylot, J.T.; Bullock, B.; Slawson, T.R.; Woodson, S.C. Blast response of lightly attached concrete masonry unit walls. *J. Struct. Eng.* **2005**, *131*, 1186–1193. [CrossRef]
19. Johnson, C.F.; Slawson, T.R.; Cummins, T.K.; Davis, J.L. Concrete masonry unit walls retroftted with elastomeric systems for blast loads. In Proceedings of the 24th Army Science Conference, Orlando, FL, USA, 29 November–2 December 2004.
20. Irshidat, M.; Al-Ostaz, A.; Cheng AH, D.; Mullen, C. Nanoparticle reinforced polymer for blast protection of unreinforced masonry wall: Laboratory blast load simulation and design models. *J. Struct. Eng.* **2011**, *137*, 1193–1204. [CrossRef]
21. Wu, G.; Ji, C.; Wang, X.; Gao, F.; Zhao, C.; Liu, Y.; Yang, G.-L. Blast response of clay brick masonry unit walls unreinforced and reinforced with polyurea elastomer. *Def. Technol.* **2022**, *18*, 643–662. [CrossRef]
22. Ji, L.; Wang, P.; Cai, Y.; Shang, W.; Zu, X. Blast Resistance of 240 mm Building Wall Coated with Polyurea Elastomer. *Materials* **2022**, *15*, 850. [CrossRef] [PubMed]
23. Yu, Q.; Zeng, D.; Xu, X.; Li, S.; Dong, W.; Dai, L. Experimental and numerical investigation of polymer-reinforced and normal autoclaved aerated concrete masonry walls under large TNT explosive loads. *Int. J. Impact Eng.* **2022**, *164*, 104188. [CrossRef]
24. Hoemann, J.M.; Dacidson, J.S.; Dinan, R.J.; Bewick, B. *Boundary Connection Behavior and Connection Design for Retrofitted Unreinforced Masonry Walls Subjected to Blast Loads*; DTIC: Fort Belvoir, VA, USA, 2010.
25. Wang, J.G. *Experimental and Numerical Investigation of Clay Brick Masonry Walls Strengthened with Spray Polyurea Elastomer under Blast Loads*; University of Science and Technology of China: Hefei, China, 2017.
26. Livermore Software Technology Corporation (LSTC). *LS-DYNA Keyword User's Manual*; LSTC: Livermore, CA, USA, 2014.
27. CSCEC Northeast Design and Research Institute Co., Ltd. *Code for Design of Masonry Structures*; Architecture Press: Beijing, China, 2011.
28. Liu, G.Q.; Shi, C.X.; Liu, Y.B. Analyses of the Elastic Modulus Values of Masonry. *J. Hunan Univ. Nat. Sci.* **2008**, *4*, 29–32.